2024 Tenth Indian Control Conference (ICC)
9 - 11 December, 2024
IISER Bhopal, India

Nonlinear Control Law for Path Following by UAVs

Sayantan Pal[1] and Sikha Hota[2]

Abstract— **This work finds a solution to reduce the convergence time by proposing a nonlinear guidance law for path following problems of Unmanned Air vehicles (UAVs). The guidance law has been derived based on the assumption that a virtual target tracks the desired path accurately and the UAV tries to catch the virtual target, that is, the relative distance between them and the look angle are made to zero. The proposed guidance law provides a generic solution which is applicable for any path-following problem. Comparative results showcase the efficacy of the proposed guidance law in terms of convergence time.**

Index Terms- Path following; Nonlinear control; Fixed-time stable system; Unmanned Aerial Vehicles.

I. INTRODUCTION

The human civilization is in the era of UAVs. The majority of typical UAV missions necessitates following a predetermined geometric trajectory [1]. Vector field guidance is one of the widely used path-following technique for autonomous vehicles. It uses vector fields (VFs) to indicate flow directions, enabling the vehicle to follow the desired path. The straight line and circular path following for UAVs using this technique was proposed in [2]. Zhou et al. [3] enhanced the above-said technique by integrating adaptive control to handle unknown wind disturbances. Lawrence proposed the Lyapunov Vector Field Guidance (LVFG) law [4] for target loitering, which was later adapted for waypoint following via dynamic switching between VFs [5]. Another variant, Tangent plus LGVF, introduced in [6], showed faster convergence for standoff targets. Pothen et al. [7] developed a curvature-constrained LGVF, achieving faster convergence including curvature limits. Harinarayana et al. [8] addressed waypoint following using straight-line convergence with LVFG. Recently, an arc-sine based VF [9] has been introduced for straight-line and circular path following, which also considered the curvature limit.

Various path-following methods have been studied in the literature using the virtual target point (VTP) technique. Examples include the Carrot-chasing algorithm [10], Pure pursuit [11], Line-of-sight (LOS) [12], Non-Linear guidance law (NLGL) [13], and Trajectory shaping guidance law [14]. The Pure pursuit guidance law [11] is effective in following straight-line paths, but its performance substantially deteriorates when it comes to curved paths. The LOS guidance law [12] directs UAVs towards the line-of-sight, with convergence rate influenced by the navigation gain of the guidance law. In the NLGL path-following technique [13], the lateral acceleration is dependent on both the distance between the VTP and the UAV, and the heading error. Ratnoo et al. [14] proposed the Trajectory Shaping guidance law, in which lateral acceleration is dependent on the instantaneous LOS angle to the VTP, the heading angles of both the UAV and the virtual target, and the estimation of time-to-go. Another VTP based tangential guidance law was proposed in [15], where the UAV kept an equal and opposite lead angle to the virtual target with respect to the LOS angle.

Several linear controllers e.g. PID and linear quadratic regulator (LQR) are extensively used for autonomous vehicle path following. These traditional methods frequently fail to produce desirable outcomes due to their linear characteristics. A detailed survey of the modeling and control of UAVs utilising PID was presented in [16]. Kukreti et al. [17] introduced an adaptive technique to tune the LQR controller, allowing it to effectively track the desired path even amidst wind disturbances. In [18], an alternative adaptive LQR controller utilizing an infinite horizon regulator strategy specifically designed for high wind flights was proposed.

To address the limitations associated with linear controllers, a nonlinear control strategy was proposed in [19] for achieving trajectory tracking and collision avoidance by multi-copters. Sliding mode control is another robust controller that is well-recognised in the field of UAV path following control. A nonlinear sliding surface-based controller that is particular to lateral track error control was proposed in [20]. Bouadi et al. [21] developed a sliding mode controller tailored to path tracking, considering the dynamics of UAVs. Alessandretti et al. [22] employed Model Predictive Control (MPC) to derive the desired linear and angular velocities to follow the desired path by fixed-wing UAVs. An alternative method achieves the same objective by employing a Lyapunov function based controller based on the target pursuit principle [23]. Recently, the work has been expanded in [24] by incorporating a fixed-time stable system in the presence of wind. The method offers a simple implementation that does not require curvature characteristics of the desired paths.

In this work, we have improved the work proposed in [24] by adopting the concepts of [25] to achieve quite considerable reduction in convergence time.

[1]Sayantan Pal, Research Scholar, Department of Aerospace Engineering, Indian Institute of Technology Kharagpur 721302, India sayantanmech94@kgpian.iitkgp.ac.in

[2]Sikha Hota, Associate Professor, Department of Aerospace Engineering, Indian Institute of Technology Kharagpur 721302, India. sikhahota@aero.iitkgp.ac.in

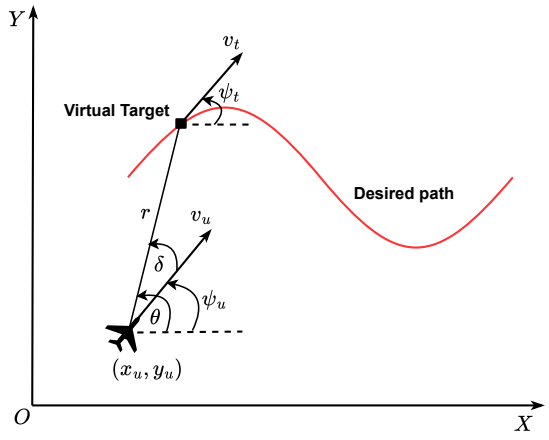


Fig. 1: Geometry of UAV path following problem

II. PROBLEM STATEMENT AND BACKGROUND

A. Model Description

The problem is to devise a guidance law for fixed-wing UAVs to follow a geometric path without prior knowledge of the curvature characteristics of the desired path. In addition, the guidance law should be independent of the initial position and orientation of the UAV and how to reduce the convergence time than those of the work available in the existing literature. The UAV is assumed to be a point-mass vehicle capable of maintaining a constant altitude. Consequently, this situation results in a planar engagement. Assuming that the UAV is initially positioned at $P(x_i, y_i)$ within a fixed coordinate frame, oriented at an angle ψ_i. The position and the heading angle at any instance are considered as (x_u, y_u) and ψ_u. Hence, the kinematic equations governing the motion of the fixed-wing UAV can be written as:

$$\begin{aligned} \dot{x}_u &= v_u \cos\psi_u \\ \dot{y}_u &= v_u \sin\psi_u \\ \dot{\psi}_u &= \omega_u \end{aligned} \tag{1}$$

where, v_u and ω_u denote the linear and angular velocities of the UAV, respectively, which serve as the control inputs. $Q(x_t, y_t)$ and ψ_t are the position and the heading angle, respectively, of the virtual target on the desired path. Analogous to the kinematics of the UAV, the equations of motion for the virtual target can be expressed as:

$$\begin{aligned} \dot{x}_t &= v_t \cos\psi_t \\ \dot{y}_t &= v_t \sin\psi_t \\ \dot{\psi}_t &= \omega_t \end{aligned} \tag{2}$$

where, v_t and ω_t represent the linear and angular velocities of the virtual target, respectively. The schematic representation of the UAV and the virtual target in the path following scenario is depicted in Fig. 1, in which r represents the LOS distance and θ denotes the LOS angle. $\delta = \theta - \psi_u$ is the look angle, which is the angle between the velocity vector of the UAV and the LOS vector.

B. Preliminary Lemmas

Consider the following dynamic system

$$\dot{x} = f(x(t)) \tag{3}$$

where, $x \in \mathbb{R}^n$, the nonlinear function, $f(x(t)) : \mathbb{R}^n \to \mathbb{R}^n$ and $x(0) = x_0 \in \mathbb{R}^n$. Assume that the origin is an equilibrium point. The following definitions and lemmas are provided from the literature, which are required to solve the problem.

Definition 1 [26]. The origin of a system (3) is said to be finite time stable if it is globally asymptotically stable and any solution of $x(t, x_0)$ of (3) reaches equilibrium at some finite time moment i.e., $\forall t \geq T(x_0) : x(t, x_0) = 0$, where $T(x_0) : \mathbb{R}^n \to \mathbb{R}^+ \cup 0$ is the settling time function.

Definition 2. [26] The origin of a system (3) is said to be fixed time stable if it is globally finite time stable with bounded settling time function $T(x_0)$, i.e. there exists $T_{max} > 0$ such that $T(x_0) < T_{max}, \forall x_0 \in \mathbb{R}$.

Lemma 1 [26]. If there exists a continuous radially unbounded and positive definite function $V(x)$ such that $\dot{V}(x) \leq -\alpha V^q(x) - \beta^p(x)$, for some $\alpha,\ \beta > 0,\ q > 1,\ 0 < p < 1$, then the origin of this system (3) is globally fixed time stable and the settling time function T can be estimated by

$$T < T_{max} := \frac{1}{\alpha(q-1)} + \frac{1}{\beta(1-p)} \tag{4}$$

Lemma 2 [25]. Consider the following scalar system

$$\dot{x} = -\xi(x)(\alpha x^p + \beta x^\lambda)^k,\ x \in \mathbb{R},\ x_0 = x(0) \tag{5}$$

where, $\xi(x) = a + (1-a)\exp(-b\|x\|^c)$ and $\lambda = \frac{1}{2k} + \frac{1}{2}q + (\frac{1}{2}q - \frac{1}{2k})\text{sgn}(\|x\| - 1)$. $a > 1,\ b \in \mathbb{R}_+,\ c \in \mathbb{R}_+,\ \alpha \in \mathbb{R}_+,\ \beta \in \mathbb{R}_+,\ p \in \mathbb{R}_+,\ q \in \mathbb{R}_+$ and $k \in \mathbb{R}_+$ are scalars with $pk < 1$ and $qk > 1$. Then the system (5) is fixed time stable for any initial value x_0, and the settling time is $T \in \mathbb{R}_+$, i.e., $x(t) \equiv 0$ for $t \geq T$, where T is bounded by

$$T < T_{max} := \frac{1}{\beta^k(qk-1)} + \frac{1}{\beta^k(1-pk)} \ln\left(1 + \left(\frac{\beta}{\alpha}\right)^k\right) \tag{6}$$

From (4) and (6), it is seen that the convergence rate is faster in [25] than that of the fixed-time stable system in [26].

III. SOLUTION APPROACH

The objective is to guide the UAV along the desired path by reducing the relative distance and the look angle to zero. To converge to the virtual target it is assumed that $v_u > v_t$. To ensure the UAV moves towards the virtual target, its heading angular rate must align with the LOS rate. To derive the guidance law, the dynamics of the LOS distance and the LOS angle are considered as the same as in [23].

The dynamics of the LOS distance between the UAV and the virtual target is given by

$$\dot{r} = v_t \cos(\theta - \psi_t) - v_u \cos(\theta - \psi_u) \tag{7}$$

The dynamics of the LOS angle of the UAV with respect to the virtual target is given by

$$\dot{\theta} = \frac{1}{r}(v_u \sin(\theta - \psi_u) - v_t \sin(\theta - \psi_t)) \tag{8}$$

In order to make the LOS distance zero, a linear velocity controller for the UAV is developed as detailed in Theorem 1.

Theorem 1. Consider the kinematic equations for the UAV and the virtual target as in (1) and (2), respectively, and the dynamics of the relative distance between the UAV and the virtual target in (7). If the UAV exerts a linear velocity,

$$v_u = \frac{1}{\cos(\theta-\psi_u)}(v_t\cos(\theta-\psi_t)+\eta_1(\kappa_1 r^{m_1}+\nu_1 r^{\gamma_1})^{k_1}) \quad (9)$$

where, $\eta_1 = a_1+(1-a_1)\exp(-b_1\|r\|^{c_1})$ and $\gamma_1 = \frac{1}{2k_1}+\frac{1}{2}n_1+(\frac{1}{2}n_1-\frac{1}{2k_1})\text{sgn}(\|r\|-1)$, $a_1>1$, $b_1\in\mathbb{R}_+$, $c_1\in\mathbb{R}_+$, $\kappa_1\in\mathbb{R}_+$, $\nu_1\in\mathbb{R}_+$, $m_1\in\mathbb{R}_+$, $n_1\in\mathbb{R}_+$ and $k_1\in\mathbb{R}_+$ are scalars with $m_1k_1<1$ and $n_1k_1>1$, then, the UAV approaches to the virtual target in a fixed time,

$$T_1 < \frac{1}{\nu_1^{k_1}(n_1k_1-1)}+\frac{1}{\nu_1^{k_1}(1-m_1k_1)}\ln\left(1+\left(\frac{\nu_1}{\kappa_1}\right)^{k_1}\right) \quad (10)$$

Proof. Let us consider a Lyapunov candidate, $V_1 = r$. By differentiating V_1 w.r.t. time and utilizing (7), we obtain

$$\dot{V}_1 = \dot{r} = v_t\cos(\theta-\psi_t)-v_u\cos(\theta-\psi_u) \quad (11)$$

Using the expression of the linear speed, v_u (9), we get

$$\begin{aligned}\dot{V}_1 &= -\eta_1(\kappa_1 r^{m_1}+\nu_1 r^{\gamma_1})^{k_1}\\ &= -\eta_1(\kappa_1 V_1^{m_1}+\nu_1 V_1^{\gamma_1})^{k_1}\end{aligned} \quad (12)$$

where, $\eta_1 = a_1+(1-a_1)\exp(-b_1\|r\|^{c_1})$ and $\gamma_1 = \frac{1}{2k_1}+\frac{1}{2}n_1+(\frac{1}{2}n_1-\frac{1}{2k_1})\text{sgn}(\|r\|-1)$. $\dot{V}_1$ is negative for some $a_1,b_1,c_1,k_1,\kappa_1,\nu_1,m_1,n_1>0$, satisfying $m_1k_1<1$ and $n_1k_1>1$. Based on the findings in *Lemma 2*, it can be concluded from (12) that the UAV meets the virtual target on the desired path within the fixed time as in (10).

Now to make the look angle (δ), zero, the following theorem is developed.

Theorem 2. Consider the kinematic equations for the UAV and the virtual target as in (1) and (2), respectively. If the UAV has an angular velocity,

$$\begin{aligned}\omega_u =& \frac{v_t}{r}(\tan\delta\cos(\theta-\psi_t)-\sin(\theta-\psi_t))\\ &+\frac{\tan\delta}{r}\eta_1(\kappa_1 r^{m_1}+\nu_1 r^{\gamma_1})^{k_1}\\ &+\eta_2(\kappa_2|\delta|^{m_2}+\nu_2|\delta|^{\gamma_2})^{k_2}\text{sign}(\delta)\end{aligned} \quad (13)$$

where, $\eta_2 = a_2+(1-a_2)\exp(-b_2\|\delta\|^{c_2})$ and $\gamma_2 = \frac{1}{2k_2}+\frac{1}{2}n_2+(\frac{1}{2}n_2-\frac{1}{2k_2})\text{sgn}(\|\delta\|-1)$, $a_2>1$, $b_2\in\mathbb{R}_+$, $c_2\in\mathbb{R}_+$, $\kappa_2\in\mathbb{R}_+,\nu_2\in\mathbb{R}_+$, $m_2\in\mathbb{R}_+$, $n_2\in\mathbb{R}_+$ and $k_2\in\mathbb{R}_+$ are scalars with $m_2k_2<1$ and $n_2k_2>1$, then, the look angle will become zero within a fixed time,

$$T_2 < \frac{1}{\nu_2^{k_2}(n_2k_2-1)}+\frac{1}{\nu_2^{k_2}(1-m_2k_2)}\ln\left(1+\left(\frac{\nu_2}{\kappa_2}\right)^{k_2}\right) \quad (14)$$

Proof. Let us consider a Lyapunov candidate, $V_2 = |\delta|$. By differentiating V_2 w.r.t. time and utilizing (8), we obtain

$$\begin{aligned}\dot{V}_2 &= \dot{\delta}\text{sign}(\delta)\\ &= (\dot{\theta}-\dot{\psi}_u)\text{sign}(\delta)\\ &= \left(\frac{1}{r}(v_u\sin(\theta-\psi_u)-v_t\sin(\theta-\psi_t))-\omega_u\right)\text{sign}(\delta)\end{aligned} \quad (15)$$

Using the angular velocity, ω_u (13) command, we get

$$\begin{aligned}\dot{V}_2 =& (\frac{1}{r}(v_u\sin(\theta-\psi_u)-v_t\sin(\theta-\psi_t))\\ &-\frac{v_t}{r}(\tan\delta\cos(\theta-\psi_t)-\sin(\theta-\psi_t))\\ &-\frac{\tan\delta}{r}(\eta_1(\kappa_1 r^{m_1}+\nu_1 r^{\gamma_1})^{k_1})\\ &-(\eta_2(\kappa_2|\delta|^{m_2}+\nu_2|\delta|^{\gamma_2})^{k_2}\text{sign}(\delta)))\text{sign}(\delta)\end{aligned} \quad (16)$$

Using v_u (9) into (16), results in

$$\begin{aligned}\dot{V}_2 =& (\frac{1}{r}((v_t\cos(\theta-\psi_t)+\eta_1(\kappa_1 r^{m_1}+\nu_1 r^{\gamma_1})^{k_1})\tan(\delta)\\ &-v_t\sin(\theta-\psi_t))-\frac{v_t}{r}(\tan\delta\cos(\theta-\psi_t)-\sin(\theta-\psi_t))\\ &-\frac{\tan\delta}{r}\eta_1(\kappa_1 r^{m_1}+\nu_1 r^{\gamma_1})^{k_1}\\ &-\eta_2(\kappa_2|\delta|^{m_2}+\nu_2|\delta|^{\gamma_2})^{k_2}\text{sign}(\delta))\text{sign}(\delta)\end{aligned} \quad (17)$$

Performing algebraic simplifications, the following can be obtained:

$$\begin{aligned}\dot{V}_2 &= -\eta_2(\kappa_2|\delta|^{m_2}+\nu_2|\delta|^{\gamma_2})^{k_2}\\ &= -\eta_2(\kappa_2 V_2^{m_2}+\nu_2 V_2^{\gamma_2})^{k_2}\end{aligned} \quad (18)$$

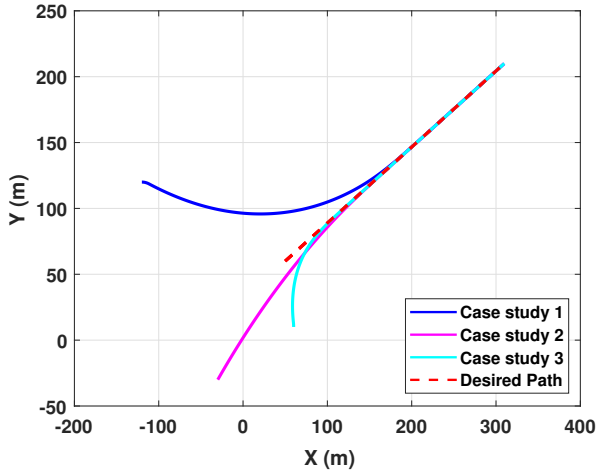
where, $\eta_2 = a_2+(1-a_2)\exp(-b_2\|\delta\|^{c_2})$ and $\gamma_2 = \frac{1}{2k_2}+\frac{1}{2}n_2+(\frac{1}{2}n_2-\frac{1}{2k_2})\text{sgn}(\|\delta\|-1)$. $\dot{V}_2$ is negative for some $a_2,b_2,c_2,k_2,\kappa_2,\nu_2,m_2,n_2>0$, satisfying $m_2k_2<1$ and $n_2k_2>1$. Drawing from the insights of *Lemma 2*, it can be inferred from (18) that the look angle approaches to zero within the fixed time as given in (14).

IV. SIMULATION RESULTS

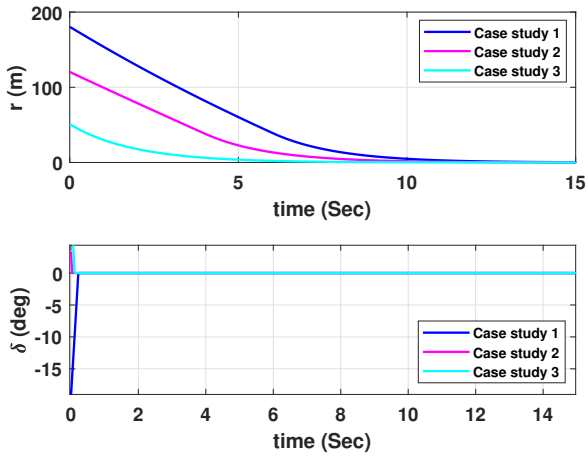
The simulations are performed in MATLAb 2020b, using the kinematic models (1) and (2) of the nonholonomic UAV and virtual target, respectively. To incorporate actuator constraints in real-world scenarios, it is assumed that the linear and angular velocities are saturated when they exceed the maximum limits. For linear velocity, we consider $v_{u_{max}} = \pm 40$ m/sec, while for angular velocity, $\omega_{u_{max}} = \pm 1.5$ rad/sec. The findings obtained from the simulations are presented in the following subsections.

A. Straight-Line Path Following

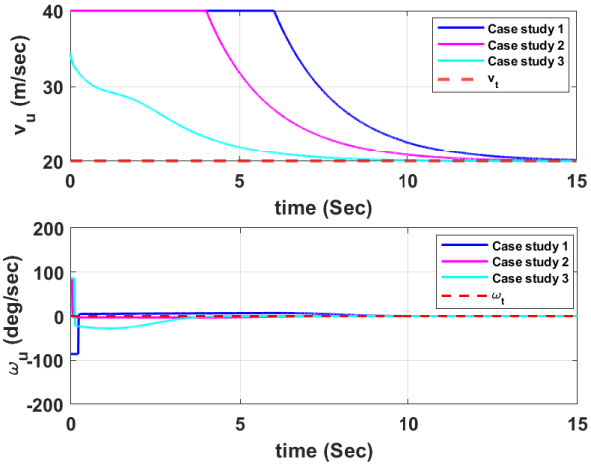
The virtual target is moving with a constant velocity of 20 m/sec and the heading angle is $\pi/6$ rad. Its initial position is Q = (50 m, 60 m). Three case studies are considered for the simulation to demonstrate the efficacy of the proposed guidance law. Each case corresponds to a different initial



(a) Trajectory of the UAV and the desired path



(b) Relative distance between the UAV and the path (r), and the look angle (δ)



(c) Linear and angular velocity of the UAV

Fig. 2: Straight line path following of UAV for different initial positions and orientations

position and orientation of the UAV, as follows: (i) P = (-120 m, 120 m), $\psi_i = 0$ rad, (ii) P = (-30 m, -30 m), $\psi_i = \pi/4$ rad, and (iii) P = (60 m, 10 m), $\psi_i = \pi/2$ rad. The design parameters are selected as $\kappa_1 = 0.3$, $\nu_1 = 0.1$, $\kappa_2 = 40$, $\nu_2 = 40$, $a_1 = 1.5$, $b_1 = 1.5$, $a_2 = 1.5$, $b_2 = 1.5$, $k_1 = 1$, $k_2 = 1$, $m_1 = 0.8$, $m_2 = 0.8$, $n_1 = 1.2$, $n_2 = 1.2$, $c_1 = 1$ and $c_2 = 1$. Fig. 2a depicts the trajectory of the UAV, and Fig. 2b shows the relative distance (distance between the UAV and the virtual target) and the look angle. The linear speed and angular speed profiles for each case are shown in Fig. 2c. The simulation study illustrates that regardless of the initial distance between the UAV and the virtual target, the UAV will ultimately follow the desired path. Notably, the convergence time remains consistent across different cases, demonstrating the nature of global convergence. This stands in contrast to asymptotic or finite-time controllers, whose efficacy relies on the initial positions and orientations of the UAV.

B. Curved Path Following

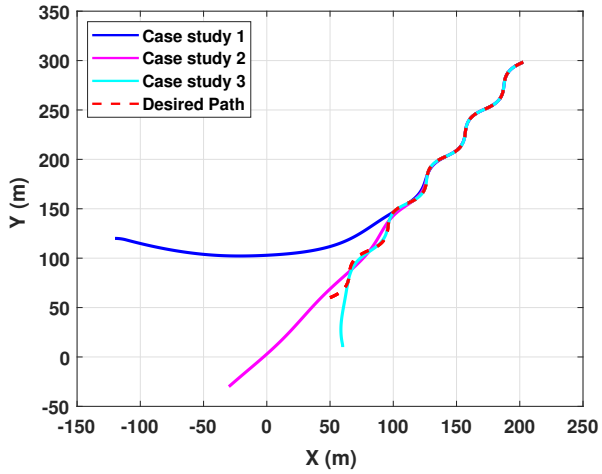
Here also the same initial conditions of the UAV are considered as the straight-line path following. The desired path is defined by the trajectory of the virtual target, which moves at a velocity of $v_t = 20$ m/sec and has an angular rate of $\omega_t = \sin(\frac{2}{3}\pi t)$ rad/sec. The initial position of the virtual target and the design parameters are considered the same as those in the straight-line path-following scenario. Figs. 3a, 3b, and 3c illustrate the trajectory of the UAV, the relative distance (between the UAV and the virtual target), the look angle, and the linear and angular speed profiles for each case, respectively. The simulation findings highlight that irrespective of the initial separation between the UAV and the virtual target, the UAV eventually adheres to the desired path.

TABLE I: Simulation parameters for comparision

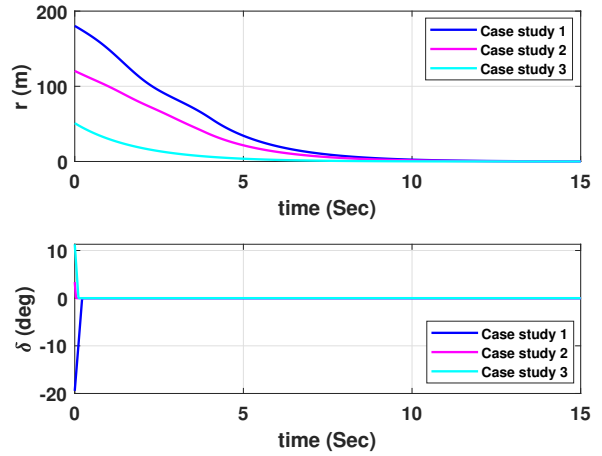
Proposed guidance	***Kumar et al.***	***Singh et al.***	***Ha et al.***
$\kappa_1 = 0.3, \nu_1 = 0.1,$	$\mathscr{M}_1 = 0.3,$	$\mathscr{M}_0 = 0.3,$	$k_1 = 0.8,$
$\kappa_2 = 40, \nu_2 = 40,$	$\mathscr{N}_1 = 0.1,$	$\mathscr{N}_0 = 40,$	$k_2 = 1.2,$
$a_1 = 1.5, b_1 = 1.5,$	$\mathscr{M}_2 = 40,$		$k_3 = 1.8$
$a_2 = 1.5, b_2 = 1.5,$	$\mathscr{N}_2 = 40,$		
$k_1 = 1, k_2 = 1,$	$\alpha_1 = 1.2,$		
$m_1 = 0.8, m_2 = 0.8,$	$\beta_1 = 0.8,$		
$n_1 = 1.2, n_2 = 1.2,$	$\alpha_2 = 1.2,$		
$c_1 = 1, c_2 = 1$	$\beta_2 = 0.8$		

V. COMPARISION

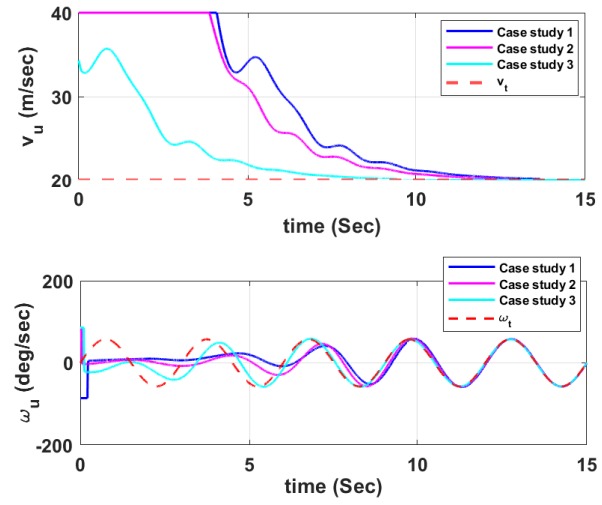
This section presents a comparative study between the proposed guidance law and existing laws proposed in [19], [23], and [24]. The study considers a curved path following where the virtual target moves with an angular velocity of $\omega_t = \cos(\pi t)$ rad/sec and a linear velocity of $v_t = 20$ m/sec, with an initial position at Q = (0 m, 0 m). The initial position and orientation of the UAV are considered as P = (50 m, -60 m), $\psi_i = \pi/2$ rad. TABLE I displays the parameters used for comparison. Fig. 4 illustrates the simulation results for



(a) Trajectory of the UAV and the desired path



(b) Relative distance between the UAV and the path (r), and the look angle (δ)



(c) Linear and angular velocity of the UAV

Fig. 3: Curve path following of UAV for different initial positions and orientations

all the guidance laws that follow the desired path. Based on Figs. 4b and 4c, it can be seen that the proposed guidance law reduces the convergence time considerably compared to other existing guidance laws.

VI. CONCLUSION

In this study, a nonlinear guidance law is proposed to follow the desired path using a virtual target approach. The proposed guidance law is computationally efficient and does not need prior information of the path curvature characteristics, facilitating a more adaptable solution to any path-following problem. The simulation results for both straight-line and curved paths clearly demonstrate the efficacy of the proposed guidance law. The comparative study concludes that the proposed nonlinear guidance law surpasses other algorithms in terms of convergence time. Future work includes extending this research to three-dimensional environments.

REFERENCES

[1] S. Pal and S. Hota, "Time-optimal bezier curves for straight-line and circular path convergence 3d space," in *2023 Ninth Indian Control Conference (ICC)*. IEEE, 2023, pp. 365–370.

[2] D. R. Nelson, D. B. Barber, T. W. McLain, and R. W. Beard, "Vector field path following for miniature air vehicles," *IEEE Transactions on Robotics*, vol. 23, no. 3, pp. 519–529, 2007.

[3] B. Zhou, H. Satyavada, and S. Baldi, "Adaptive path following for unmanned aerial vehicles in time-varying unknown wind environments," in *2017 American Control Conference (ACC)*. IEEE, 2017, pp. 1127–1132.

[4] D. Lawrence, "Lyapunov vector fields for uav flock coordination," in *2nd AIAA" Unmanned Unlimited" Conf. and Workshop & Exhibit*, 2003, p. 6575.

[5] D. Lawrence, E. Frew, and W. Pisano, "Lyapunov vector fields for autonomous uav flight control," in *AIAA Guidance, Navigation and Control Conference and Exhibit*, 2007, p. 6317.

[6] H. Chen, K. Chang, and C. S. Agate, "Tracking with uav using tangent-plus-lyapunov vector field guidance," in *2009 12th International Conference on Information Fusion*. IEEE, 2009, pp. 363–372.

[7] A. A. Pothen and A. Ratnoo, "Curvature-constrained lyapunov vector field for standoff target tracking," *Journal of Guidance, Control, and Dynamics*, vol. 40, no. 10, pp. 2729–2736, 2017.

[8] T. Harinarayana, S. V. Krishnan, S. Hota, and R. Kushwaha, "A lyapunov guidance vector field based continuous curvature path generation for waypoint following of uavs," in *2021 International Conference on Unmanned Aircraft Systems (ICUAS)*. IEEE, 2021, pp. 498–506.

[9] A. Shivam and A. Ratnoo, "Arcsine vector field for path following guidance," *Journal of Guidance, Control, and Dynamics*, vol. 46, no. 12, pp. 2409–2420, 2023.

[10] X. Jin, W. Mei, and Y. Zhaolong, "Path following control for unmanned aerial vehicle based on carrot chasing algorithm and plos," in *2020 IEEE International Conference on Artificial Intelligence and Information Systems (ICAIIS)*. IEEE, 2020, pp. 571–576.

[11] T. Yamasaki, H. Takano, and Y. Baba, "Robust path-following for uav using pure pursuit guidance," in *Aerial Vehicles*. IntechOpen, 2009.

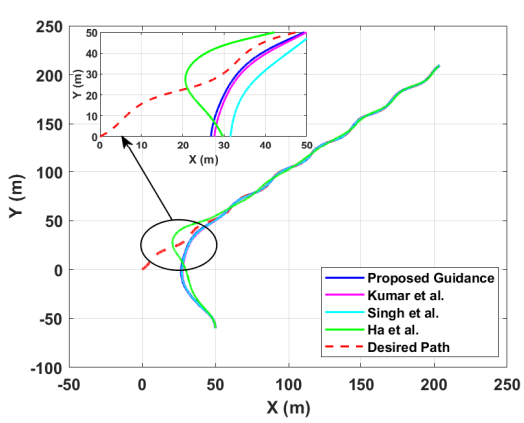
[12] R. Rysdyk, "Uav path following for constant line-of-sight," in *2nd AIAA" Unmanned Unlimited" Conf. and Workshop & Exhibit*, 2003, p. 6626.

[13] S. Park, J. Deyst, and J. How, "A new nonlinear guidance logic for trajectory tracking," in *AIAA guidance, navigation, and control conference and exhibit*, 2004, p. 4900.

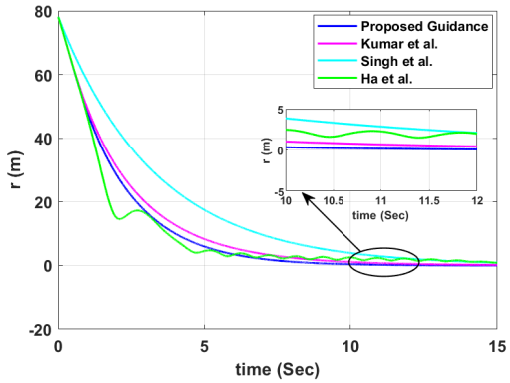
[14] A. Ratnoo, S. Y. Hayoun, A. Granot, and T. Shima, "Path following using trajectory shaping guidance," *Journal of Guidance, Control, and Dynamics*, vol. 38, no. 1, pp. 106–116, 2015.

[15] S. Thakar and A. Ratnoo, "A tangential guidance logic for virtual target based path following," in *AIAA Guidance, Navigation, and Control Conference*, 2017, p. 1042.

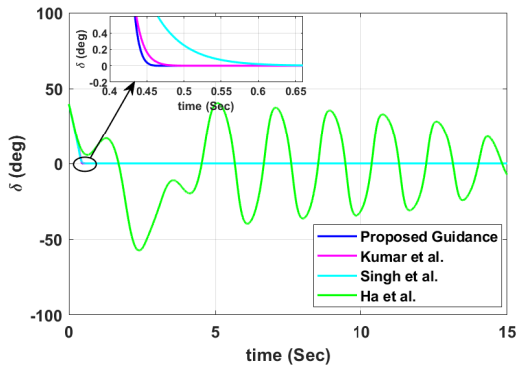
[16] I. Lopez-Sanchez and J. Moreno-Valenzuela, "Pid control of quadrotor uavs: A survey," *Annual Reviews in Control*, vol. 56, p. 100900, 2023.



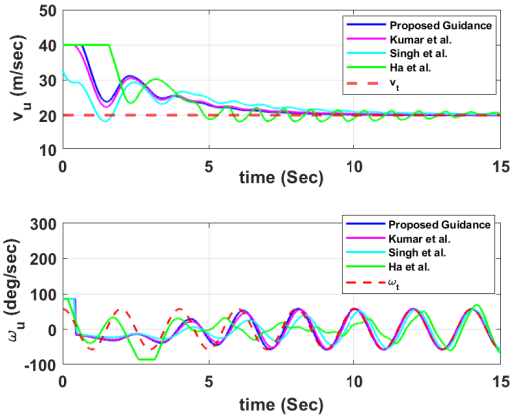
(a) Trajectory of the UAV and the desired path



(b) Relative distance between the UAV and the path



(c) Look angle



(d) Linear and angular velocity of the UAV

Fig. 4: Comparision study with existing algorithms for curve path following of UAV

[17] S. Kukreti, M. Kumar, and K. Cohen, "Genetically tuned lqr based path following for uavs under wind disturbance," in *2016 International Conference on Unmanned Aircraft Systems (ICUAS)*. IEEE, 2016, pp. 267–274.

[18] A. Ratnoo, P. Sujit, and M. Kothari, "Adaptive optimal path following for high wind flights," *IFAC Proceedings Volumes*, vol. 44, no. 1, pp. 12 985–12 990, 2011.

[19] L. N. N. T. Ha, D. H. P. Bui, and S. K. Hong, "Nonlinear control for autonomous trajectory tracking while considering collision avoidance of uavs based on geometric relations," *Energies*, vol. 12, no. 8, p. 1551, 2019.

[20] M. Z. Shah, R. Samar, and A. I. Bhatti, "Guidance of air vehicles: A sliding mode approach," *IEEE Transactions on Control Systems Technology*, vol. 23, no. 1, pp. 231–244, 2014.

[21] H. Bouadi, M. Bouchoucha, and M. Tadjine, "Sliding mode control based on backstepping approach for an uav type-quadrotor," *World Academy of Science, Engineering and Technology*, vol. 26, no. 5, pp. 22–27, 2007.

[22] A. Alessandretti and A. P. Aguiar, "A planar path-following model predictive controller for fixed-wing unmanned aerial vehicles," in *2017 11th international workshop on robot motion and control (RoMoCo)*. IEEE, 2017, pp. 59–64.

[23] S. K. Singh, A. Sinha, and S. R. Kumar, "Nonlinear control design for an unmanned aerial vehicle for path following," *IFAC-PapersOnLine*, vol. 55, no. 1, pp. 592–597, 2022.

[24] S. Kumar, A. Sinha, and S. R. Kumar, "Robust path-following guidance for an autonomous vehicle in the presence of wind," *Aerospace Science and Technology*, p. 109225, 2024.

[25] L. Cao, B. Xiao, and M. Golestani, "Robust fixed-time attitude stabilization control of flexible spacecraft with actuator uncertainty," *Nonlinear Dynamics*, vol. 100, pp. 2505–2519, 2020.

[26] A. Polyakov, "Nonlinear feedback design for fixed-time stabilization of linear control systems," *IEEE transactions on Automatic Control*, vol. 57, no. 8, pp. 2106–2110, 2011.